P1.9

A ONE-SEASON ASSIMILATION AND IMPACT STUDY OF NESDIS AND NAVY'S WINDSAT RETRIEVED DATA IN THE NCEP GLOBAL DATA ASSIMILATION SYSTEM

Li Bi* [1,3] James A. Jung [1,2] Michael C. Morgan [3] John F. Le Marshall [4]

[1] Cooperative Institute for Meteorological Satellite Studies, Univ. of WI-Madison
[2] Joint Center for Satellite Data Assimilation & Univ. of MD-College Park, 5200 Auth Rd, Camp Springs, MD 20746
[3] Atmospheric and Oceanic Sciences, Univ. of WI-Madison
[4] Centre for Australian Weather and Climate Research (CAWCR), Australia

1. INTRODUCTION

Sea surface wind vectors have been estimated with active remote sensing instruments, such as QuikSCAT (Yu and McPherson 1984), and have been proven to have a positive impact on forecasts. Passive polarimetric microwave radiometry is being introduced as an alternative vector wind measurement approach to the active remote sensing approach of QuikSCAT and other instrument. As a result WindSat, a space-based multi-frequency polarimetric microwave radiometer (Gaiser et al., 2004), was developed by the Naval Research Laboratory for the U.S. Navy and the National Polar-orbiting Operational Environmental Satellite System (NPOESS) Integrated Program Office (IPO). The projected capabilities of the WindSat mission are to demonstrate spaceborne remote sensing of ocean surface wind vectors (speed and direction). Wind direction measurement with polarimetric instruments, which sense the polarity of light, can also demonstrate how ocean surface properties change with wind and boundary layer conditions. WindSat will aid with forecasting short-term weather, issuing timely weather warnings and gathering general climate data. WindSat wind vectors have been proven to have a positive impact on forecasts in the Southern Hemisphere (Le Marshall et al, 2006).

2. BACKGROUND

2.1 WindSat

The WindSat radiometer has polarimetric channels at 10.7, 18.7 and 37.0 GHz and dual-polarization (vertical and horizontal) channels at 6.8 and 23.8 GHz. These provide information related to surface wind vectors as well as sea surface temperature, atmospheric water vapor, integrated cloud liquid water and rain rate over the ocean. Measurements of the modified stokes vector, which includes the vertical and horizontal polarizations and the third and fourth stokes parameters, provides sufficient information to retrieve the ocean wind vector (Bettenhausen et al., 2006). The 6.8GHz dual-polarized channel is more sensitive to sea surface temperature (SST) than to winds and is used to determine effects due to variations in SST. Similarly, the 23.8GHz dual-polarized channel is highly sensitive to atmospheric water vapor. Consequently, measurements at 23.8 GHz help determine the effects of atmospheric attenuation on radiation from the ocean surface.

Wind roughening the surface of the ocean causes an increase in the brightness temperature of the microwave radiation emitted from the water's surface. From the brightness temperature measured by satellite radiometers, wind speed and direction can be retrieved. The Navy's ocean surface wind vectors used in this study have been determined using a non-linear iterative optimal estimation method. Details of the scheme which uses a one layer atmospheric model and a sea surface emissivity model is found in Bettenhausen et al., (2006). The Environmental Data Records (EDRs) generated by this scheme have been put into Binary Universal Form for the Representation of meteorological data (BUFR) format at the National Oceanic and Atmospheric Administration's (NOAA) National Center for Environmental Prediction (NCEP) in preparation for operational use. The Naval Research Laboratory (NRL) WindSat Version 2 wind vector retrieval algorithm is used in this study (Bettenhausen et al., 2006).

The National Environmental Satellite, Data, and Information Service (NESDIS) WindSat retrieved wind vectors used in this study is based on the NOAA/NESDIS WindSat's wind vector retrieval algorithm. This algorithm utilizes an empirical model function that establishes relationship between the third and fourth Stokes parameters and the surface winds truth (Jelenak et al. 2004).

2.2 Global Data Assimilation System

For these experiments, the NCEP GDAS/GFS (Global Data Assimilation/Forecast System) was used. A horizontal resolution of 382 spectral triangular waves (T382) were used with 64 vertical layers. The most recent information about the GFS atmospheric model is available from NCEP (or

* Corresponding author address: Li Bi, Univ. of Wisconsin-Madison, 1225 W. Dayton St. Madison, WI 53706; email: bi1@wisc.edu

online at http://www.emc.ncep.noaa.gov/officenotes/newernotes/on442.pgf) The analysis scheme is a three-dimensional variational data assimilation (3DVAR) scheme and is referred to as the Gridpoint Statistical Interpolation (GSI) (Derber et al. 1991; Derber et al. 2003).

3. EXPERIMENTAL DESIGN

In collaboration with Joint Center for Satellite Data Assimilation (JCSDA), studies have been done to evaluate the impact of assimilating both NESDIS WindSat data and Navy's WindSat data in the NCEP GDAS/GFS. A March 2007 version of the GSI and GFS were used and running at a 1 degree superob for both NESDIS and Navy's WindSat data at T328L64. The time period studied is from 15 February to 30 March, 2007.

Some Qualify Control (QC) for WindSat data has been done in the retrieval process. Observations that are flagged for rain, land, sun glint, RFI (Radio Frequency Interference) or sea ice contamination are omitted. WindSat processing uses the median filtering technique to smooth the final wind field (Bettenhausen et al., 2006).The NCEP GDAS model wind fields are used for WindSat processing initialization.

The additional quality control investigation that we conducted the experiments with WindSat data includes: (a) Data used at 6 hour synoptic times with a plus/minus 3 hour window; (b) all observations over land, near coast, over ice and potentially rain contaminated are rejected before superobing; (c) if the absolute value of the superobed wind component is more than 6ms^{-1} from the corresponding background wind component the observation is rejected; (d) any superobed observations that are over 20ms^{-1} and less than 4ms^{-1} are removed.

After finalizing the quality control, three runs were undertaken to test and compare the attributes of using the NESDIS WindSat data and the Navy WindSat data to a control experiment. The control experiment contains all the operational data used during the period and includes all of the real time data cutoff requirements. The three experiments include: (a) A GFS experiment with all data types (control) (b) a GFS experiment including Navy WindSat retrieval data, and (c) a GFS experiment including NESDIS WindSat retrieval data. For this poster, forecast impact comparisons will be presented from assimilating the Navy's WindSat and NESDIS WindSat data to a benchmark or control experiment.

All diagnosis presented here exclude the first 15 days of the time period. (Zapotocny et al. 2007) This delay in evaluating the statistics allows for the impact of the WindSat data to be added from the model initial conditions. Excluding the first 15 days reduce the one season window to 30 days. The forecast impact diagnostics for this paper were also terminated at 96 h to concentrate on the short term forecast impact.

Once the 30 day WindSat experiments were completed, several diagnostics were performed on the archived data. The traditionally anomaly correlation statistics were performed using the traditional NCEP algorithms (NWS 2006). The anomaly correlation is defined as the correlation between the predicted and analyzed anomalies of the variables.

In addition to the anomaly correlation statistics traditionally performed by NCEP, another diagnostic used here is the geographic distribution of forecast impact (FI) explained in Zapotocny et al. (2005a) and Zapotocny et al. (2007). For this one season assimilation and impact study, a series of two-dimensional FI results are shown at different levels. The geographic distribution of FI for a specific level is calculated using:

$$FI(x,y) = 100\mathrm{X}\left\{\left(\sqrt{\frac{\sum_{i=1}^{N}(\mathrm{C}i-\mathrm{A}i)^2}{\mathrm{N}}}-\sqrt{\frac{\sum_{i=1}^{N}(\mathrm{E}i-\mathrm{A}i)^2}{\mathrm{N}}}\right)\Big/\sqrt{\frac{\sum_{i=1}^{N}(\mathrm{C}i-\mathrm{A}i)^2}{\mathrm{N}}}\right\}$$

The variables *C* and *E* are the control and experiment forecasts, respectively. The variable *A* is the GDAS experiment analysis containing all data types, which is valid at the same time as for forecasts. *N* is the number of diagnostic days.

Another diagnostic used here is the area weighted Root Mean Square Error (RMS) calculation discussed by Zapotocny et al. (2007). The area weighted RMS calculation accounts for the reduction in area as for grid boxes approach the poles. The area weighting function is defined as:

$$A_i^{'} = A_i \times \frac{\sin(\phi_i + \frac{\Delta}{2}) - \sin(\phi_i - \frac{\Delta}{2})}{2\sin(\frac{\Delta}{2})}$$

where ϕ is the latitude of the grid box and Δ is the resolution of the grid box. The numerator is the relative size of the grid box. The denominator is the relative size of the grid box at the equator (Zapotocny et al, 2007).

Figure 1 displays a preliminary comparison of the RMS and bias by bins for Navy WindSat and NESDIS WindSat from WindSat runs using either NESDIS or Navy WindSat data. Panel (a) shows the results from Navy WindSat and panel (b) shows the results from NESDIS WindSat. There is large RMS and bias for NESDIS WindSat retrieved wind for wind speed which is less than 4ms^{-1}.

The differences between control analysis and Navy's WindSat analysis are also calculated for the magnitude of wind speed and sea level pressure (SLP). Figure 2 illustrate a snapshot for the wind speed difference (top panel) and SLP difference (bottom panel). The magnitude of wind speed difference can be as large as over 8ms^{-1} and SLP difference as large as 3hPa. The figure displays the snapshot of 0Z March 1, 2007.

4. RESULTS

The Anomaly Correlation (AC) comparisons are presented in Figure 3. The results presented in Figure 3 show the 500 hPa day 5 geopotential height anomaly correlation from a control run and two WindSat experiments using the Gridpoint Statistical Interpolation (GSI) and a version of forecast model from March 2007. The best (highest) anomaly correlations are achieved using the Navy's retrieved WindSat winds at 1000 hPa for both hemispheres and at 500 hPa in the Northern Hemisphere. Although not shown, other fields such as 1000 hPa wind also benefit somewhat from the addition of Navy's WindSat data.

Figure 4 displays geographic distributions of 1000 hPa forecast impact averaged over March 2007 for u component of the Navy WindSat retrieved winds at 0.9950 sigma level at forecast hours (a) 6, (b) 12, (c) 24, and (d) 48. The range of FI is from -50 to 100. The 0.9950 sigma level is the level which is closest to where the WindSat wind observations are added to the assimilation system. Of the four fields shown, the largest impacts are in Africa, South America and Australia at 6-hour forecast. By 12 hour, the impacts in South American and Australia decrease with the largest impact are still realized over Africa. There is a marked decrease in forecast impact by 24 hour and further decreases are diagnosed at 48 hour.

The area weighted RMS comparison between Navy WindSat experiment and control experiment are presented in Figure 5. The left panel is the comparison for u component of the winds and the right panel is for v component of the winds at 10m. The analysis from the experiment is used in this calculation. At 6 hour forecast, the area weighted RMS for Navy WindSat experiment has smaller RMS value than the control run. By 24 hour, the difference decrease and further decrease are diagnosed at 48 hour.

5. SUMMARY

Key findings of the experiments completed thus-far, some of which extend beyond the results presented here, are that:

- Preliminary results indicate that Navy WindSat improved the forecast at mid-latitudes.
- The NESDIS WindSat improved the forecasts in the tropics.
- The NESDIS version has more slow wind speed observations which generally have greater O-B errors.
- The Navy WindSat data has positive FI at the surface which means the Navy WindSat experiment forecast compares more favorably to its corresponding analysis with the WindSat data included
- From the area weighted RMS calculation, the RMS value for Navy WindSat experiment is smaller than the control run starting at 6 hour.

6. ACKOWLEDGEMENTS

The authors wish to thank Dr. Tom Zapotocny for leading this project. It is with great sadness that he passed away. The authors wish to thank Stephen Lord (NCEP) for computer resources and tape space. The authors also wish to thank Peter Gaiser and Zorana Jelenak for providing the Navy and NESDIS WindSat data. The authors also wish to thank Dennis Keyser and Stacie Bender for collecting and processing our various data streams. The authors also wish to thank the JCSDA for the computer time required for this study. This research was supported under NOAA grant NA07EC0676 which supports JCSDA activities.

7. REFERENCES

Bettenhausen, M.H., Smith, C.K., Bevilacqua, R.M., Wang, N., Gaiser, P.W., and S. Cox, 2006: A Non-linear Optimization Algorithm for Wind sat Wind Vector Retrievals. *IEEE Trans. Geosci. Remote Sens.,* **44**, 597-610.

Derber, J. C., D. F. Parrish, and S. J. Lord, 1991: The New Global Operational Analysis System at the National Meteorological Center. *Wea. Forecasting*, **6**, 538-547.

Derber , J. C., Van Delst, P., Su, X. J., Li, X., Okamoto, K. and Treadon, R. 2003: Enhanced use of radiance data in the NCEP data assimilatioin system. *Proceedings of the 13th International TOVS Study Conference*. Ste. Adele, Canada, 20 October – 4 November, 2003.

Gaiser, P.W., St. Germain , K.M., Twarog, E.M., Poe, G.A., Purdy, W., Richardson, D., Grossman, W., Jones, W.L., Spencer, D., Golba, G., Cleveland, J., Choy, L., Bevilacqua, R.M., and P.S. Chang, 2004: The WindSat spaceborne polarimetric microwave radiometer: Sensor description and early orbit performance. *IEEE Trans. Geosci. Remote Sens.,* **42**, 2347-2361.

Le Marshall, J., Bi, L., Jung, J., Zapotocny, T. and Morgan, M. 2006. WindSat Polarimetric Microwave Observations Improve Southern Hemisphere Numerical Weather Prediction**.** *Aust. Meteor. Mag.* **56,** 35-40**.**

Jelenak, Z., T. Mavor, L. Connor, N.-Y. Wang, P.S. Chang, and P. Gaiser (2004): Validation of ocean wind vector retrievals from WindSat polarimetric measurements, presented at *The 4th Int. Asian-Pacific Environmental Remote Sensing Conf.*

NWS, cited 2006: NCEP Anomaly Correlations. [Available online from http://wwwt.emc.ncep.noaa.gov/gmb/STATS/STATS.html .]

Yu, T.-W., and R. D. McPherson, 1984: Global Data Assimilation Experiments with Scatterometer Winds from Seasat-A. *Mon. Wea. Rev.*, **112**, 368-376. *

Zapotocny, T., W. P. Menzel, J. A. Jung, and J. P. Nelson III, 2005: A Four Season Impact Study of Rawinsonde, GOES and POES Data in the Eta Data Assimilation System. Part I: The Total Contribution. *Wea. Forecasting*, **20**, 161-177.

Zapotocny, T., J. A. Jung, J. F. Le Marshall and Treadon, R. 2007: A Two-Season Impact Study of Satellite and In Situ data I the NCEP Global Data Assimilation System. *Wea. Forecasting*, **22**, 887-909.

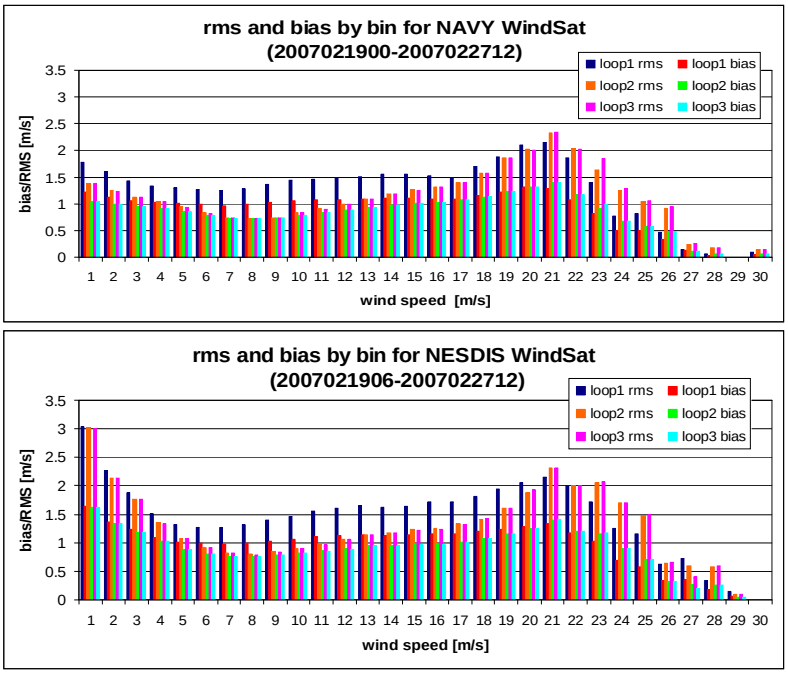

Figure 1. A preliminary comparison of the rms and bias by bin for Navy WindSAT and NESDIS WindSAT from WindSAT runs using either NESDIS or Navy WindSAT data. Panel (a) shows the results from Navy WindSAT and panel (b) shows the results from NESDIS WindSat.

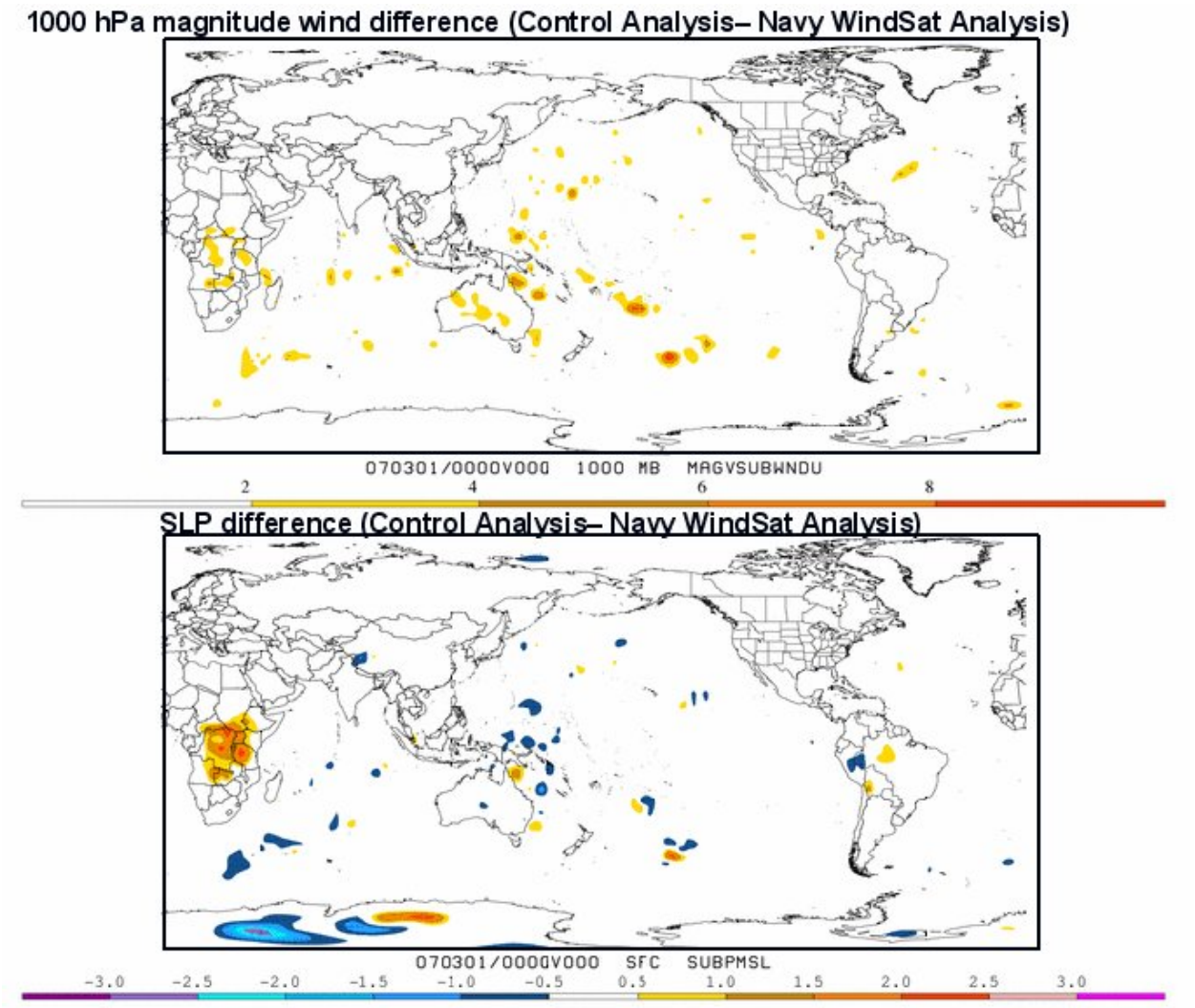

Figure 2. 1000hPa wind speed difference and SLP difference between control analysis and Navy's WindSat analysis at 0Z March 1, 2007.

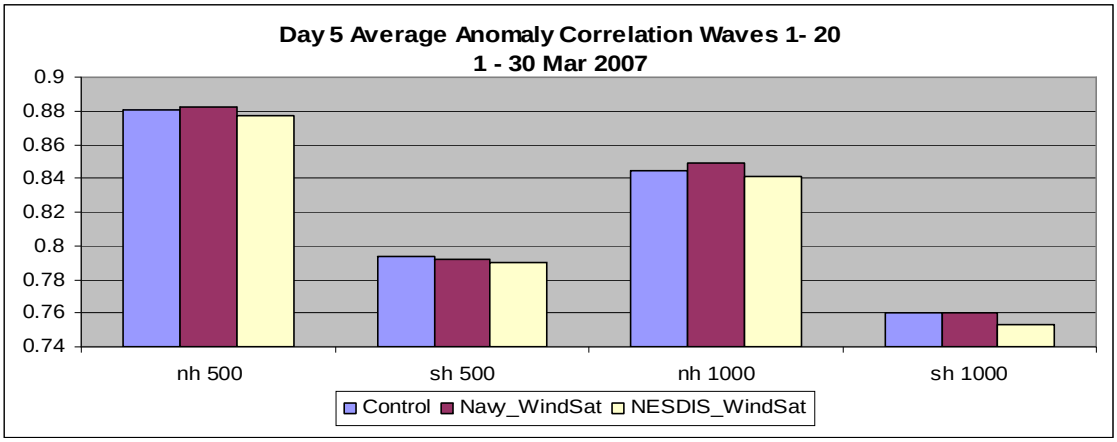

Figure 3. Three-way comparison of the Day 5 Geopotential height anomaly correlation for the period 1 – 30 March 2007.

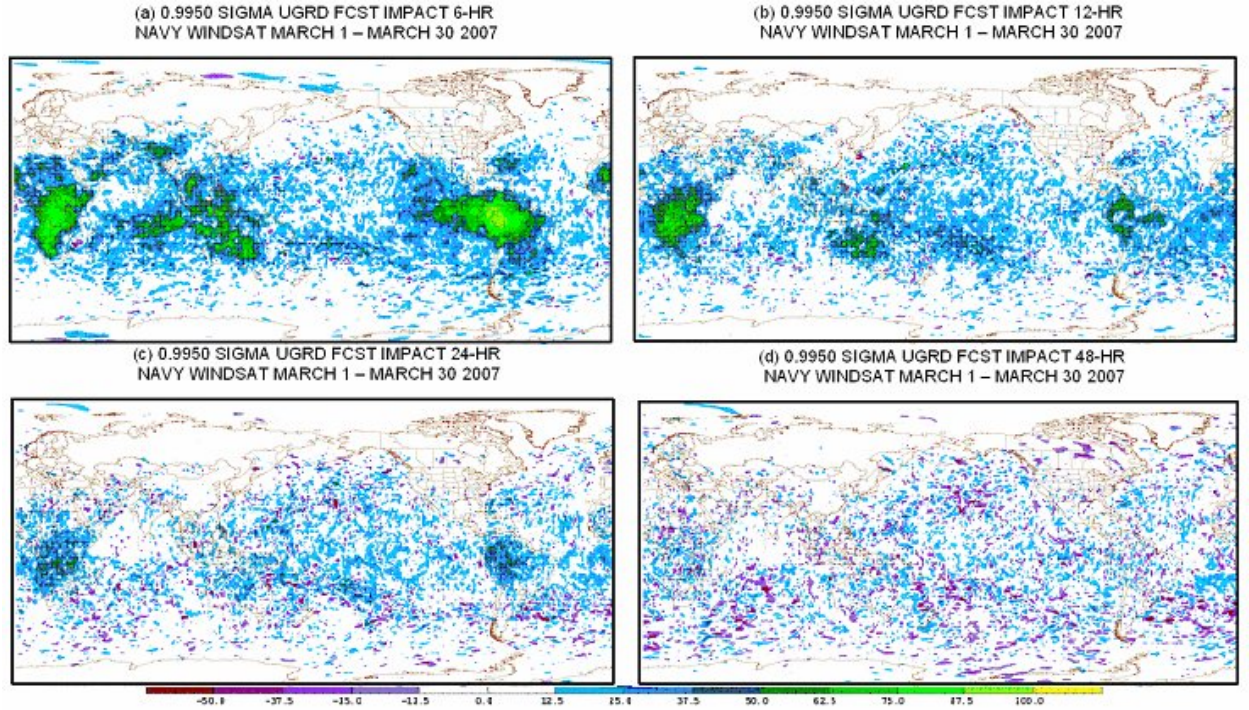

Figure 4. Geographic distribution of forecast impact from March 1 to March 30 for u component of the wind at 0.9950 sigma level for Navy WindSat retrieved winds at forecast hours (a) 6, (b) 12, (c) 24, and (d) 48. The range of forecast impact is from -50 to +100.

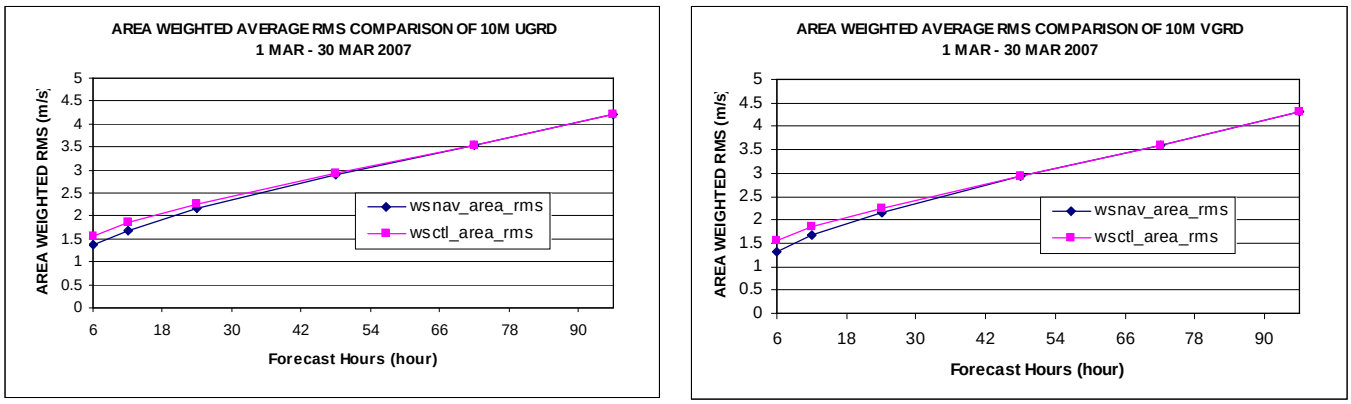

Figure 5. Area weighted average RMS comparison of 10m u component and v component for Navy's WindSat experiment and control run from March 1 to March 30, 2007.